Proceedings of the 8th International Conference on MicroManufacturing
University of Victoria, Victoria, BC, Canada, March 25-28, 2013

Effect of the tool locus on the cutting thickness in the ball endmill process

ICOMM 2013 **No.** 91

Takenori ONO[1]
[1]Takenori ONO; Dep. of Mechanical Engineering, Kyushu Sangyo Univ., Japan; tono@ip.kyusan-u.ac.jp

Key Words: Ball Endmill, Cutting Thickness, Tool Attitude.

BACKGROUND

The need for micro fabrication on glass materials, for example a chemical inspection plate and micro molding die, has been increasing. Glass machining is one potential approach for micro fabrications. It can realize more effective and safer operation than the conventional manner such as etching process [1-3]. Many studies have tried to cut glass with a shaping process to observe the cutting phenomenon. However, this process cannot achieve a high machining rate because the cutting depth is restricted to less than a micrometer to perform ductile mode cutting. Other approaches such as the milling process have been studied to achieve a high production rate with increasing flexibility compared with the shaping process [4,5]. The author has proposed a glass cutting with a small -diameter milling tool (ex. Fig. 1) and reported machining characteristics that are evaluated by cutting experiments[6,7]. With optimal cutting conditions, micro milling can machine the glass material without a brittle cracking as shown in Fig. 2.

Recently, the author is investigating the effect of a tool edge roughness on the brittle cracking in glass milling. The previous experiments showed that brittle cracking is affected by the tool edge roughness[8]. It is concluded that the edge roughness changes conditions of tool engagement and material stress distribution. In this study, cutting experiments are performed by a mono-crystal diamond milling tool with which edge roughness is re-dressed as the artificial "roughness" shape by focused ion beam machine tool. To evaluate the change in cutting thickness by a re-dressed tool, the author has proposed the calculation method of cutting thickness in the ball endmill process in previous announcements [9]. This method can simulate the change in cutting thickness which takes into account edge roughness and tool attitude. The method, however, can only calculate the change in thickness in straight grooving because the tool attitude and feed direction are assumed as the constant. The free-form surface is machined by the ball endmill process and the attitude of milling tool is changed by the cutter locus. For example, in the milling process by a multi-axis control machining center, although the cutting tool is fixed on the machining coordinate by the spindle head, the attitude of the ball endmill is changed by the motion of motor stages. The cutting thickness is changed by the tool attitude and motion and a cutting condition such as a cutting force is also changed. To evaluate the change in cutting thickness in the cutting process of free-form surfaces, a numerical calculation method is developed for cutting thickness which takes into account change in tool

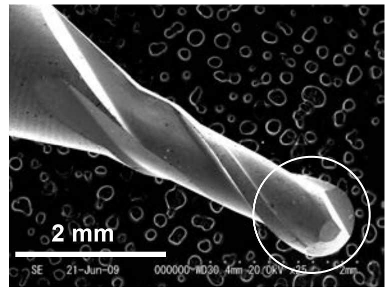

(a) Carbide ball endmill

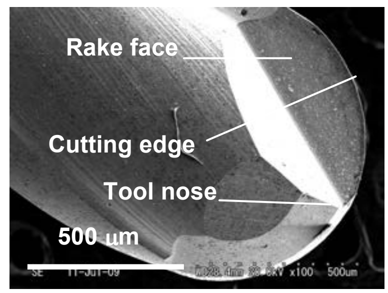

(b) Tool edge

Fig. 1: Carbide ball endmill

Specifications: material, carbide; radius of curvature, 0.5 mm; neck length, 2.9 mm; helix angle, 30 deg; and coat material, TiAlN.

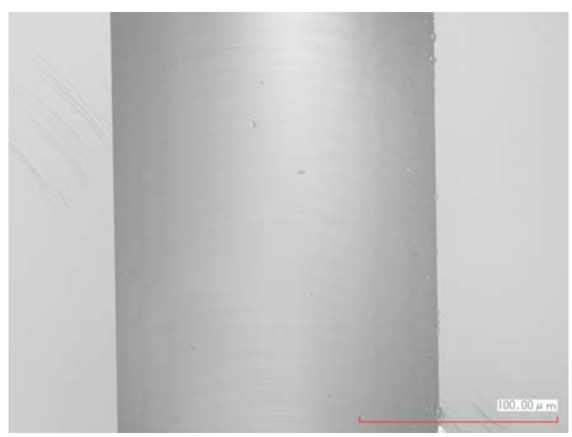

Fig. 2: Surface machined by carbide ball endmill

Cutting conditions: Tool, R0.5 TiAlN coated ball endmill; material cut, soda lime glass; feed rate, 0.48 mm/min; rotational speed, 20000 rpm; feed rate per edge, 12 nm/edge; cutting speed, 31.4 m/min; depth of cut, 50 μm; and lubrication, water.

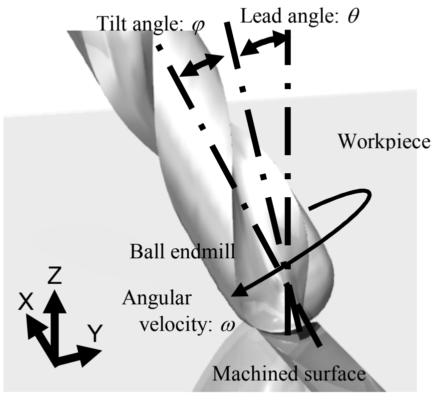

(a) Tool inclination in milling process

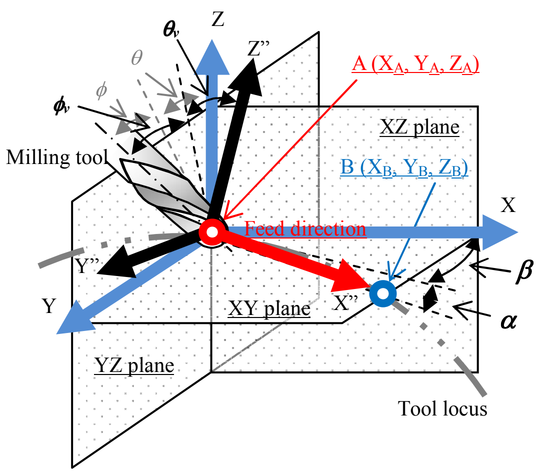

(b) Tool attitude at locus

Fig. 3: Change in tool attitude by locus

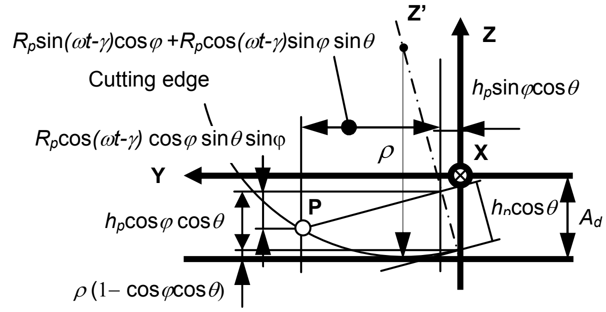

(a) Viewed from feed direction (X)

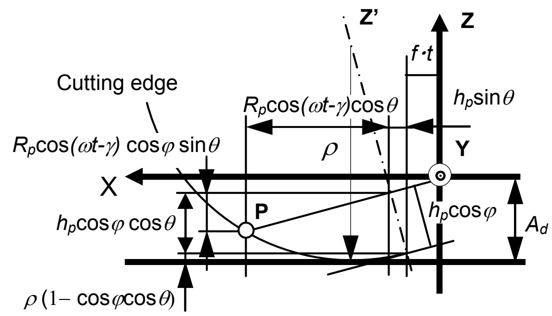

(b) Viewed from Y-axis

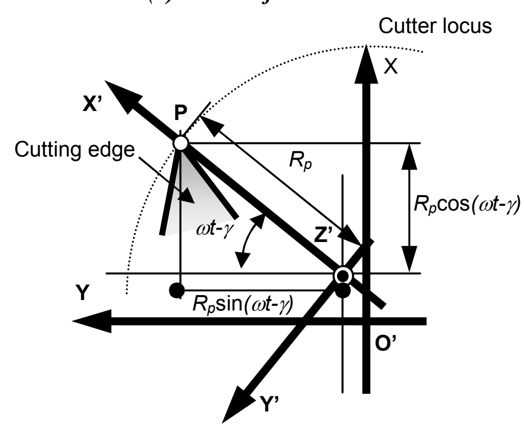

(c) Viewed from inclined rotational axis Z`

Fig. 4: Geometry of milling process with inclined ball endmill

attitude and tool locus. This report proposes a new-developed method and discusses the calculation results with the proposed method.

CALCULATION METHOD FOR CALCULATING CUTTING THICKNESS

Fig. 3 shows the motion of a ball endmill in the milling process. In the new-developed method, the milling tool is fixed on the coordinate system of the machine tool (described as X, Y, Z) at any posture and the tool attitude changes by the tool locus. As shown in Fig. 3, the fixed milling tool inclines to +X direction of the coordinate system of the machine tool X-Y-Z at a lead angle of θ and to +Y direction at a tilt angle of φ, respectively. The milling tool with the nose radius ρ is then fed to +X direction of the machine tool coordinate system at a feed rate of f and rotational speed of ω, respectively. In this situation, the tool attitude in machine coordinate (X_t, Y_t, Z_t) is described by the following equations:

$$\begin{cases} X_t = \sin\theta \\ Y_t = \cos\theta\cdot\sin\phi \\ Z_t = \cos\theta\cdot\cos\phi \end{cases} \tag{1}$$

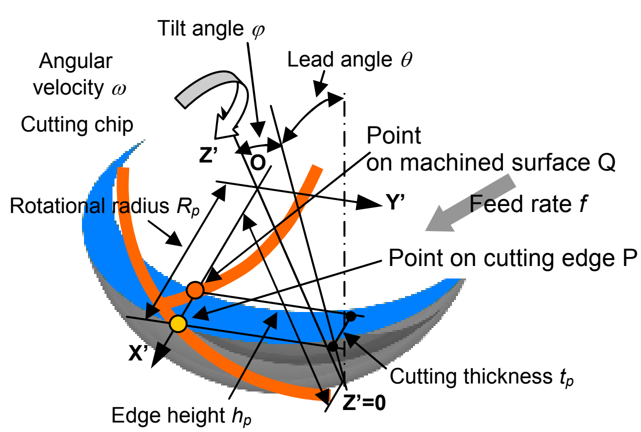

Fig. 5: Schematic of chip removal in the milling process

If the center of the ball nose moves from point A (X_A, Y_A, Z_A) to point B (X_B, Y_B, Z_B) as shown in Fig. 3, the angles of tool locus (vector $\overrightarrow{AB}$) α *and* β are described by the following equations:

$$\begin{cases} \alpha = \tan^{-1}\left(\dfrac{Z_B - Z_A}{\sqrt{(X_B - X_A)^2 + (Y_B - Y_A)^2}}\right) \\ \beta = \tan^{-1}\left(\dfrac{Y_B - Y_A}{X_B - X_A}\right) \end{cases} \tag{2}$$

According to these equations, the tool attitude in the coordinate of tool locus (X”, Y”, Z”) as shown in Fig. 3 can be described as follows:

$$\begin{cases} X''_t = \cos\alpha \cdot \cos\beta \cdot X_t + \cos\alpha \cdot \sin\beta \cdot Y_t - \sin\alpha \cdot Z_t \\ Y''_t = -\sin\beta \cdot X_t + \cos\beta \cdot Y_t \\ Z''_t = \sin\alpha \cdot \cos\beta \cdot X_t + \sin\alpha \cdot \sin\beta \cdot Y_t + \cos\alpha \cdot Z_t \end{cases} \tag{3}$$

Based on Eq. (2), a lead angle of θ_v and a tilt angle of φ_v of milling tool in a coordinate of tool locus are described as follows:

$$\theta_v = \tan^{-1}\left(\frac{X''_t}{Z''_t}\right), \quad \varphi_v = \tan^{-1}\left(\frac{Y''_t}{\sqrt{X''^{\,2}_t + Z''^{\,2}_t}}\right) \tag{4}$$

If the locus in the coordinate system of the machine tool is divided by the unit time and approximately as a line, the change in tool attitude can be calculated with these equations. And the change in cutting thickness in the milling process can be simulated by a calculation method introduced in previous announcements [9]. This method calculates a change in the cutting thickness by the locus of the cutting edge at any tool attitude. Fig. 4 shows the schematics for the cutter locus in the milling process viewed along X-axis (a), Y-axis (b), and center axis of milling tool (c), respectively. In this figure, P is the point at which the cutting edge removes material. In this situation, the location of the P (X_P, Y_P, Z_P) in the machine coordinate system X-Y-Z is given as follows:

$$\begin{cases} x_p = R_p \cdot \cos\theta_v \cdot \cos(\omega t - \gamma) + h_p \cdot \sin\theta_v + f \cdot t \\ y_p = -R_p \cdot \cos\varphi_v \cdot \sin(\omega t - \gamma) \\ \qquad - R_p \cdot \sin\varphi_v \cdot \sin\theta_v \cdot \cos(\omega t - \gamma) + h_p \cdot \sin\varphi_v \cdot \cos\theta_v \\ z_p = R_p \cdot \sin\varphi_v \cdot \sin(\omega t - \gamma) \\ \qquad - R_p \cdot \cos\varphi_v \cdot \sin\theta_v \cdot \cos(\omega t - \gamma) - A_d \\ \qquad + h_p \cdot \cos\varphi_v \cdot \cos\theta_v + \rho \cdot (1 - \cos\varphi \cdot \cos\theta) \end{cases} \quad \cdots(5)$$

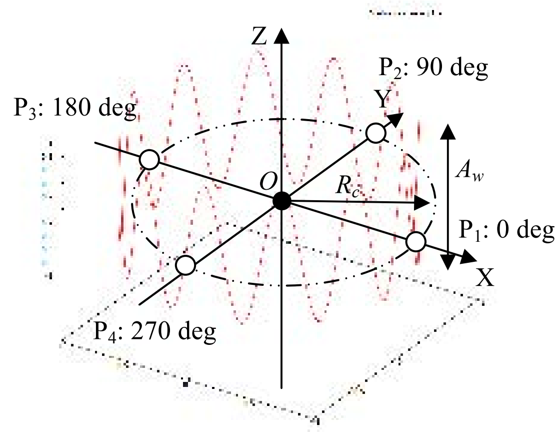

Fig. 6: Locus model in calculation tests

Table 1. Cutting conditions in calculation

Condition	Value
Number of wave period	12
Locus amplitude A_w mm	0, 0.1, 1.0
Radius of locus R_c mm	12.0
Lead angle θ deg	0, 45
Tilt angle φ deg	0, 45
Feed rate mm/min	0.48
Rotational speed rpm	20000
Lead angle $d\delta_{ij}$ deg	180
Time step sec	5 x10^{-5}

In Eq. (5), γ is the delay angle of Point P to the bottom of the cutter, t is the cutting time. Fig. 5 illustrates the schematic of a chip removing process by the inclined ball endmill. In this figure, point Q is the crossing point between the rotational radius of the P and machined surface at the previous cutting. The location of Q (X_Q, Y_Q, Z_Q) in the machine coordinate is given as follows:

$$\begin{cases} x_Q = R_Q \cdot \cos\theta_v \cdot \cos(\omega \cdot (t + \Delta t - d\delta_{ij}/\omega) - \gamma_Q) \\ \qquad + h_Q \cdot \sin\theta_v + f \cdot (t + \Delta t - d\delta_{ij}/\omega) \\ y_Q = -R_Q \cdot \cos\varphi_v \cdot \sin(\omega \cdot (t + \Delta t - d\delta_{ij}/\omega) - \gamma_Q) \\ \qquad - R_Q \cdot \sin\varphi_v \cdot \sin\theta_v \cdot \cos(\omega(t + \Delta t - d\delta_{ij}/\omega) - \gamma_Q) \\ \qquad + h_Q \cdot \sin\varphi_v \cdot \cos\theta_v \\ z_Q = R_Q \cdot \sin\varphi_v \cdot \sin(\omega \cdot (t + \Delta t - d\delta_{ij}/\omega) - \gamma_Q) \\ \qquad - R_Q \cdot \cos\varphi_v \cdot \sin\theta_v \cdot \cos(\omega(t + \Delta t - d\delta_{ij}/\omega) - \gamma_Q) \\ \qquad - A_d + h_Q \cdot \cos\varphi_v \cdot \cos\theta_v + \rho \cdot (1 - \cos\varphi_v \cdot \cos\theta_v) \end{cases} \quad \cdots(6)$$

Where Δt is the delay angle of Point P to the bottom of the cutter, t is the cutting time, and $d\delta_{ij}$ is the lead angle of the previous cutting edge for the recent cutting edge. According to these functions, the change of cutting thickness t_P in the milling process is calculated by the following:

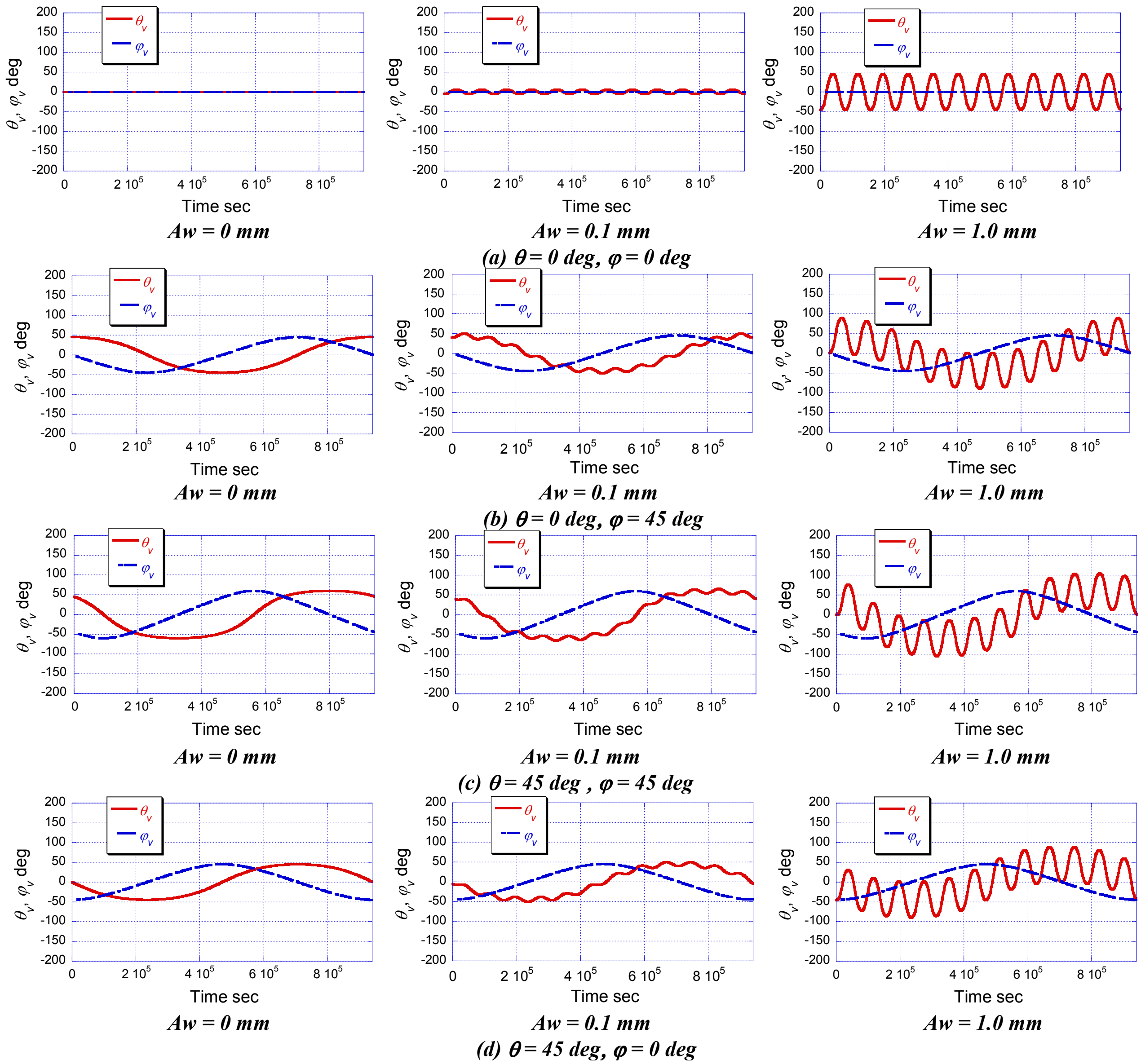

Fig. 7 Change in θ_v and φ_v by the locus amplitude A_w and tool inclination angles θ and φ

$$t_p = \overline{PQ} = R_p - [(x_Q - ft)\cos\theta_v - \{z_Q - \rho(1-\cos\theta_v)\}\sin\theta_v]\sin(\omega t - \gamma) + y_Q\cos(\omega t - \gamma) \quad \cdots(7)$$

If t_P is negative, the cutting edge does not cut the material in Eq. (7). The simulation is performed by dividing the cutting edge into small segments. The rotational radius R_p in each segment is determined with the actual (or theoretical) shape of the cutting edge. By calculating the cutting thickness at each time step with calculated tool inclination angles, the time series of the cutting thickness can be calculated in any tool locus and attitude.

CALCULATION RESULTS OF TOOL ATTITUDE

To evaluate the validity of the proposed method, the following calculation tests are performed. Fig. 6 shows the tool locus in tests. The locus is formed as the sine wave circle around the origin of the coordinate. In tests, the radius of locus R_c in Fig. 6 is 1 mm and the amplitude of sine wave A_w in Fig. 6 is changed at 0, 0.1 and 1.0 mm, respectively. And the ball endmill with a nose radius of 0.5 mm and helix angle of 30 degree is fixed on the machine tool at various inclination angles. The inclined milling tool moves along the locus at a feed rate of 0.48 mm/min, at a rotational speed of 20000 rpm corresponding to an angular velocity of 2094.4 rad/sec. The depth of groove is constant at 0.05 mm, because it is assumed that the top surface of the workpiece has the wavy shape corresponding to the tool locus in this test. The calculation is performed by a personal computer at the unit cutting time of $5x10^{-5}$ sec. Cutting conditions in calculation tests are

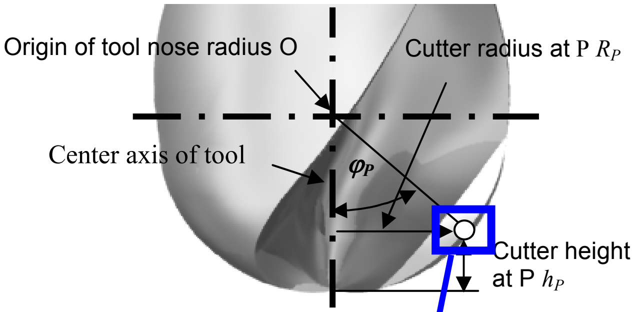

(a) Tool nose

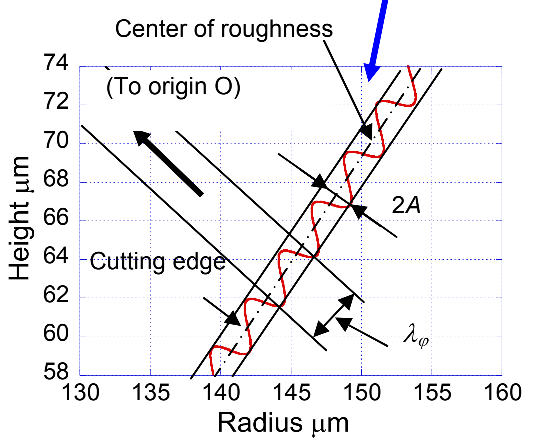

(b) Edge shape

Fig. 8: Edge shape model in numerical simulations

Table 2. Parameters of determined edge models

No.	A nm	λ_φ deg	Number of edge points
1	0.0	0.5	10000
2	500.0		

Table 3. Cutting conditions in calculation

Condition	Value
Locus amplitude A_w mm	0, 0.5, 1
Radius of curvature of endmill ρ mm	0.5
Number of cutting edges	2
Depth of cut A_d mm	0.02
Lead angle θ deg	0
Tilt angle φ deg	0, 15, 45
Time step sec	3.3 x10^{-7}

*Other cutting conditions are the same as in Table 1.

summarized in Table 1. Fig. 7 shows the time series of lead angle θ_v and tilt angle φ_v at various inclination angles and the locus amplitude A_w. As shown in Fig. 7(a), only the change in θ_v can be recognized, the change in φ_v is not recognized at

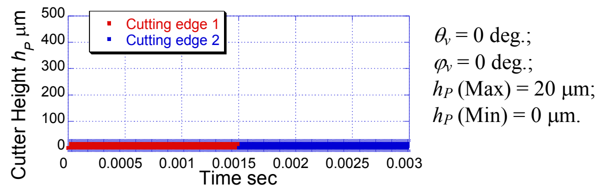

(a) Aw=0 μm

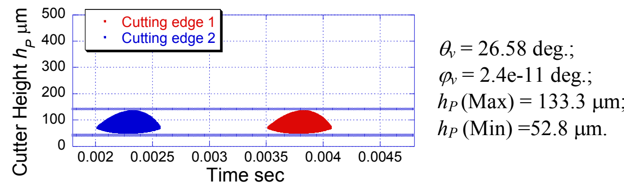

(b) Aw=0.5 μm

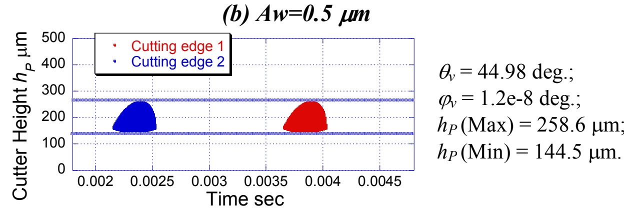

(c) Aw=1 μm

Fig. 9: Changes in the actual cutting area by the wave amplitude
Conditions: φ=0 deg.

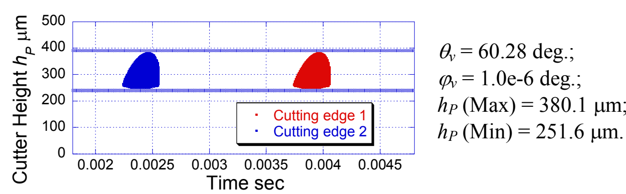

Fig. 10: Changes in the actual cutting area by the tool inclination
Conditions are the same as those in Fig. 9 (c) except the tilt angle.

the θ and φ =0, because the tool is always perpendicular to the XY plane. However, if the tool inclines in any direction as shown in Fig. 7 (b) (c) (d), the φ_v is also changed by the tool locus. At the locus amplitude A_w of 0 mm, the θ_v and φ_v are smoothly changed to correspond to the circular locus. On the other hand, if the locus amplitude is increased, a wavy change can be recognized only in the lead angle θ_v corresponding to the wavy locus since the tool feed direction is parallel to the Z direction at any time in this locus model.

CALCULATION RESULTS OF CUTTING THICKNESS

The cutting thickness is calculated with the tool locus model illustrated in Fig. 6. Calculation tests are performed with simple sine-wave edge models as shown in Fig. 8. In this figure, A is the amplitude of the sine-wave, and φ_p is the angle between the rotational radius of point P and the center axis of the tool. λ_φ is the pitch angle of the wave shape. The edge shape is described as follows:

$$\begin{cases} R_p = J(\varphi_p) = \left(\rho - A + A\cdot\sin(2\pi\varphi_p/\lambda_\varphi)\right)\cdot\sin\varphi_p \\ h_p = G(\varphi_p) = \rho - \left(\rho - A + A\cdot\sin(2\pi\varphi_p/\lambda_\varphi)\right)\cdot\cos\varphi_p \end{cases} \quad \cdots(8)$$

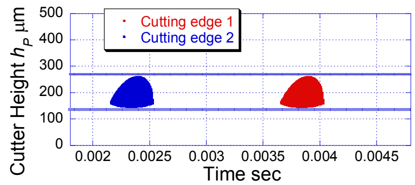

$\theta_v \sim 45.0$ deg.;
$\varphi_v = 1.0e\text{-}5$ deg.;
h_P (Max) = 259.6 µm;
h_P (Min) = 146.4 µm.

(a) 9x10-5 sec (near P_1)

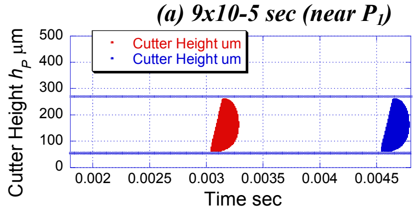

$\theta_v = 1.0e\text{-}5$ deg.;
$\varphi_v \sim 45.0$ deg.;
h_P (Max) = 259.6 µm;
h_P (Min) = 60.5µm.

(b) 3534.3 sec (near P_4)

Fig. 11: Changes in the actual cutting area by the cutting time
Conditions: Aw=1 mm, φ=45 deg.

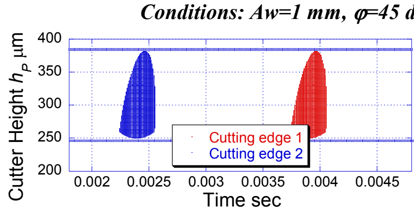

$\theta_v = 60.28$ deg.;
$\varphi_v = 1.0e\text{-}6$ deg.;
h_P (Max) = 380.1 µm;
h_P (Min) = 251.6 µm.

(a) A=0 µm

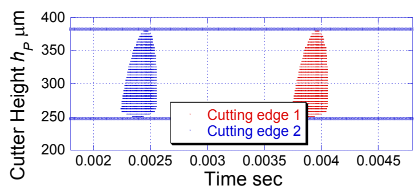

$\theta_v = 60.28$ deg.;
$\varphi_v = 1.0e\text{-}6$ deg.;
h_P (Max) = 380.1 µm;
h_P (Min) = 251.6 µm.

(b) A=1 µm

Fig. 12: Changes in the actual cutting area by the amplitude A
Conditions: Aw=1 mm, φ=0 deg.

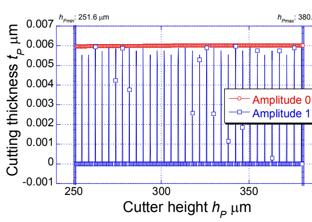

(a) Actual cutting area in h_P

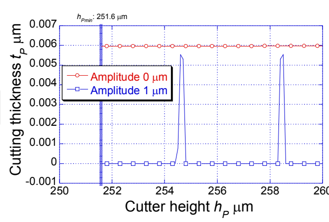

(b) Magnified view

Fig. 13: Cutting thickness on cutting edge at 9.0 x 10-5 sec
Conditions are the same as those in Fig. 12

In cutting simulations, cutting edges remove the smooth surface to determine the actual cutting area on the cutting edge and cutting thickness. The wave amplitude is changed to 0 and 500 nm the same pitch (φ_p=0.5 deg) to observe the effect of the edge roughness. Parameters of edge models and cutting conditions in the calculation tests are summarized in Table 2 and 3.

Fig. 9 shows the change in the actual cutting by the wave amplitude *Aw* at a cutting point P_1 as shown in Fig. 6. In this figure, the calculated inclination angles θ_v, φ_v and maximum and minimum cutter height h_P are also described. Although the milling tool does not incline to the Z direction, the actual cutting area is widely changed by the wave amplitude because the inclination of the tool locus to the XY plane in the machine coordinate is increased by the wave amplitude. Fig. 10 shows the actual cutting area at the tilt angle φ of 15 degrees. In this figure, other cutting conditions are those in Fig. 9 (c). In this case, the lead angle θ_v becomes about 60 degrees, corresponding to the increasing of tilt φ. Fig. 11 shows the change in the cutting area by the cutting time (9x10^{-5} sec (near P_1), 3534.3 sec (near P_4)) at φ of 45 degree and A_w of 0 µm. The actual cutting area is widely changed with inclination angles θ_v and φ_v by the tool locus, although the locus does not change in the Z direction. According these results, the new method can simulate changes in the tool attitude by changes of the tool locus and attitude.

Fig. 12 shows changes of the actual cutting area by the amplitude of cutting edge roughness *A*. In this figure, other cutting conditions are those in Fig. 10. The actual cutting area is decreased at the amplitude of 1 µm because the cutting thickness is much less than the cutting edge roughness, actual cutting is occurred only the top of the roughness wave. Fig. 13 shows change in the cutting thickness by the edge roughness at the cutting time of 9.0 x 10^{-5} sec when the maximum actual cutting area has occurred in Fig. 12. As shown in this figure, the cutting thickness partially changes by the increasing of the edge roughness corresponding to Fig. 12. According to these results, the new method can calculate the change in the cutting thickness by the change in the cutting edge roughness.

CONCLUSION

This report proposes a new-developed method and discusses the calculation results. By the proposed method, cutting thickness can be calculated which takes into account change in tool attitude and tool locus to evaluate the change in cutting thickness in the cutting process of free-form surfaces. In calculation tests, it is shown that tool attitude and actual cutting point change with the tool locus.

REFERENCES

[1] Puttick, K. E., Rudma, M. R. Smith, K. J. Franks, A., and Lindsey, K. (1989), "Single-Point Diamond Machining of Glasses," Proc. R. Soc. London, Ser. A., Vol. 426, pp. 19-30.

[2] Komanduri, R., Lucca, D. A. and Tani, Y. (1997), "Technological Advance in Fine Abrasive Processes," Annals of CIRP, Vol. 46/2, pp. 545-596.

[3] Yoshino, M., Aoki, T. and T. Shirakashi (2001), "Scratching Test of Hard-brittle Materials under Hydrostatic Pressure," Transactions of ASME, Journal of Manufacturing Science and Engineering, Vol. 123, pp.231-239.

[4] Takeuchi, Y., Sawada, S. and Sata, T. (1996), "Ultra-precision 3-D Micromachining of Glass," Ann. CIRP, 45, 11, 401.

[5] Matsumura, T., Hiramatsu, T, Shirakashi, T. and Muramatsu, T. (2004), "A Study on Cutting Force in the Milling Process of Glass," Transactions of NAMRI/SME, Vol. 32, pp.463-470.

[6] Matsumura, T., Ono, T., "Glass Machining with Ball Endmill," Transactions of NAMRI/SME, Vol. 33 (2005), pp.319-326.

[7] Ono, T. (2010), "Tool Wear Characteristics of the Micro Milling of Optical Glass," Transactions of NAMRI/SME, Vol. 38, pp.261-268.

[8] Ono, T. (2011), "Influence of Cutting Edge Roughness on Brittle Cracking in the Milling Process on Soda Lime Glass," Proceedings of NAMRC39, 4527(CD-ROM).

[9] Ono, T. (2012), "Numerical Simulation of the Micro Milling Process with Sine-wave Edge Shapes," Proceedings of ICOMM 2012, pp. 473-477.